Analysis of the $^8S_{7/2}$ to $^6P_{7/2}$ two-photon absorption transitions of Gd^{3+} in $Gd(OH)_3$ in an applied magnetic field

1989 J. Phys.: Condens. Matter 1 7385

(http://iopscience.iop.org/0953-8984/1/40/012)

J. Phys.: Condens. Matter 1 (1989) 7385–7394. Printed in the UK

Analysis of the $^8S_{7/2} \rightarrow {}^6P_{7/2}$ two-photon absorption transitions of Gd^{3+} in $Gd(OH)_3$ in an applied magnetic field

B Jacquier†, J C Gacon†, Y Salem†, C Linares† and R L Cone‡

† UA 442 du CNRS, Université Claude Bernard, Lyon 1, 69622 Villeurbanne Cédex, France

‡ Department of Physics, Montana State University, Bozeman, MT 59717, USA

Received 17 April 1989

Abstract. We report a detailed analysis of the intensity and polarisation dependence of the $^8S_{7/2} \rightarrow {}^6P_{7/2}$ two-photon transition Stark components of Gd^{3+} in the concentrated magnetic insulator $Gd(OH)_3$ under an applied magnetic field (up to 3.5 T) at very low temperature (2 K). The experimental technique consisted of detecting the ultraviolet $^6P_{7/2} \rightarrow {}^8S_{7/2}$ one-photon fluorescent emission resulting from two-photon excitation in the $^6P_{7/2}$ states, using a single pulsed dye-laser beam. The standard second-order theory of Axe is shown to fail in explaining the relative intensities of the Stark components. This is especially true in the case of the $\Delta M = 0$ transitions for which strong disagreements are observed. It is shown that the introduction of the third-order contribution involving the spin–orbit interaction within the $4f^65d$ states allows the experimental spectra to be reproduced in a correct way. Finally the effects of ion–ion interactions on the two-photon line profiles are discussed.

1. Introduction

The observation of $^8S_{7/2} \rightarrow {}^6P_J$ two-photon transitions in $Gd^{3+}:LaF_3$ by Dagenais *et al* (1981) has stirred a great theoretical interest since Axe's standard second-order theory of two-photon absorption was proved to fail in explaining the relative strengths of the transitions under question. Judd and Pooler (1982) showed that the anomalous intensities observed for the $^8S_{7/2} \rightarrow {}^6P_{7/2}$ transitions could be accounted for by expanding Axe's theory to include third-order terms involving the spin–orbit interaction among intermediate states belonging mainly to the $4f^65d$ excited configuration. Along this vein, Downer and Bivas (1983) have shown that the introduction of third- and fourth-order contributions involving spin–orbit and/or crystal-field interactions among $4f^65d$ states could explain the integrated intensities, as well as the individual Stark-component strengths, of most of the two-photon transitions induced between the $^8S_{7/2}$ ground state and excited states belonging to ^6P_J, ^6I_J and ^6D_J multiplets of Gd^{3+} in LaF_3.

Very few papers have been devoted to two-photon absorption transitions in concentrated magnetic materials in which ion–ion interactions may have drastic effects on the optical properties. Mahiou *et al* (1983) reported on the first observation of direct two-photon absorption of Gd^{3+} in $GdCl_3$. More recently, Jacquier *et al* (1987) published preliminary results on two-photon transition intensity measurements in $Gd(OH)_3$ under

0953-8984/89/407385 + 10 $02.50

an applied magnetic field. In the present paper, we report a comprehensive analysis of the experimental results for $Gd(OH)_3$. Emphasis is laid on the predominant role of the third-order scalar contribution to explain the $^8S_{7/2} \rightarrow {}^6P_{7/2}$ individual Stark-component intensities, as observed for $Gd^{3+}:LaF_3$.

The experimental results are described in § 2. Section 3 is concerned with the theoretical analysis of these results. As concluding remarks, we discuss the contribution of such two-photon spectroscopy measurements to the knowledge of the coupling between active ions in concentrated magnetic materials.

2. Experimental results

As has been known for many decades, the Gd^{3+} ion occupies a particular position in the rare earth series, since it has an f^7 half-filled configuration. Among other features, this situation implies two main consequences: (i) a ground state $^8S_{7/2}$ well isolated from the first higher energy levels ^6P_J lying more than 30 000 cm^{-1} above it; (ii) the absence of orbital angular momentum in the ground state in contrast to the next ^6P_J states, and presence of a large spin momentum. It follows that Gd^{3+} materials may exhibit unusual optical and magnetic properties. Both aspects are illustrated in the spectroscopic studies of the magnetic rare earth insulator $Gd(OH)_3$.

Needle-like $Gd(OH)_3$ single crystals were grown by Mroczkowski *et al* (1970) at Yale University. The well known hexagonal structure observed in the entire series of the rare earth hydroxides has a space group $P6_3/m$ (C^2_{6h}) where the Gd^{3+} ion occupies a non-centrosymmetric C_{3h} site with a six-hydroxide coordination number, each Gd^{3+} being surrounded by two cation nearest neighbours (NN) along the C_3 axis (c axis) and six next nearest neighbours (NNN) in diagonal planes containing the C_3 axis. Skjeltorp *et al* (1972) have shown that $Gd(OH)_3$ orders antiferromagnetically at 0.94 K with predominant nearest neighbour interactions and a residual pseudo-one-dimensional character at temperatures as high as 2.47 K. However, in an external magnetic field of 3.5 T, the Gd^{3+} spins tend to be aligned along the field providing a spin configuration similar to that of a ferromagnet.

A $Gd(OH)_3$ crystal with an optical path of 0·3 mm was immersed in the pumped helium bath of a superconducting magnet providing a fixed temperature of about 2 K with an external magnetic field applied along the c axis and varying from 0 to 4 T. Selective laser excitation was achieved with a 10 ns pulsed neodymium YAG pumped dye laser with typical peak powers greater than 1 MW (rhodamine 640 dye). Care was taken to use as low laser peak powers as possible (40 kW) to avoid heating of the sample or other possible parasitic non-linear effects. Single laser beam experiments only were performed with the light propagating perpendicular to the c axis through a Soleil–Babinet compensator and a polariser providing linearly polarised identical photons (the electric field being either parallel or perpendicular to the c axis, $\varepsilon \parallel c$ or $\varepsilon \perp c$). A laser resolution better than 0.1 cm^{-1} has been achieved, much narrower than the linewidth observed in such concentrated materials. The excitation spectra were recorded by monitoring the overall UV fluorescence selected by three UV filters (MTO H 325 a) giving a stray light ratio smaller than 10^{-10} in the visible range. Moreover, a 2 ms gated photon counting signal detection ensured a quite good signal-to-noise ratio for accumulated data of 10–50 laser shots, depending upon the strength of the fluorescence signal. Finally the accumulated photon signal was displayed on the screen of a Tektronix graphic computer.

Table 1. Experimental and calculated relative intensities of the $^8S_{7/2} \rightarrow {}^6P_{7/2}$ two-photon transitions at 2 K. $S^{(2)}_{TPA}$ and $S^{(3)}_{TPA}$ stand for the calculated strengths derived from second-order and third-order analysis (figure 3), respectively.

$^8S_{7/2}$	$^6P_{7/2}$	$\varepsilon \parallel c$			$\varepsilon \perp c$		
M	$2M'$	$S^{(2)}_{TPA}$	$S^{(3)}_{TPA}$	Exp.	$S^{(2)}_{TPA}$	$S^{(3)}_{TPA}$	Exp.
	±7	46	1544	150	17	2730	860
	±5	1	2176	480	11	2369	840
	±3	8.6	2652	1210	21	2153	1190
	±1	24	2918	770	31	2048	470

In contrast to lightly doped rare earth materials where the absorbing centres are generally the emitting ones, the optical excitation in concentrated compounds can migrate resonantly through the normal ions (often called intrinsic), due to the strength of the ion–ion interactions between excited ions and nearby non-excited ions. However, because of the presence of impurities or local strains, perturbed active ions exist that trap the optical excitation and contribute to the so-called sensitised fluorescence. Then, the fluorescence spectra of fully concentrated materials generally exhibit fast intrinsic fluorescence and retarded trap fluorescence as a result of an efficient diffusion process from intrinsic to perturbed ions. This is the case for $Gd(OH)_3$ for which the fluorescence spectrum at 2 K is composed of one intrinsic line resonant with the transition to the lowest $^6P_{7/2}$ excited state and several intense lines shifted towards lower energy with respect to the intrinsic one. As a consequence, two-photon excitation spectra could be recorded by monitoring both the intrinsic and impurity-induced trap fluorescences. Furthermore, by taking advantage of our pulsed excitation (10 Hz) and of the lifetime of the fluorescence (4 ms) we could detect signals under low pumping power, using time resolved spectroscopy techniques.

In the absence of an external magnetic field, the polarised excitation spectra at 2 K reproduce the four crystal-field components of the $^6P_{7/2}$ multiplet, the degeneracy of which is completely removed in the C_{3h} symmetry of the rare earth sites (Jacquier *et al* 1987). The positions of the peaks, which agree with the one-photon measurements, and their integrated intensities are listed in table 1. The four Stark components exhibit relative intensities with significant polarisation dependences. They have been labelled by $M' = \pm\frac{7}{2}, \pm\frac{5}{2}, \pm\frac{3}{2}, \pm\frac{1}{2}$ with respect to the increase of energy, according to measurements under an external magnetic field.

Lines profiles measured in such a concentrated material indicate a broadening of few wavenumbers (slightly smaller than that observed in the UV one-photon spectrum), in contrast to lightly doped rare earth materials (Downer and Bivas 1983). As expected, the application of an external magnetic field removes the degeneracy of each $\pm M$ level and, depending upon the polarisation of the laser beam, the number of observed lines is given by the ΔM selection rules (figure 1). However, since the $^8S_{7/2}$ ground state magnetic splitting is larger than kT, at least at 3.5 T and for temperatures close to 2 K, the intensities of the lines are strongly temperature dependent. Then, the intensity of a line attributed to a transition orginating from the M state of the ground term will be depleted by the population factor $\exp(-\Delta_M/kT)$ where Δ_M stands for the relative energy of the considered state with respect to the ground state. This also affects the one-photon excitation spectra identically (Salem *et al* 1989). Following the selection rules in § 3, we

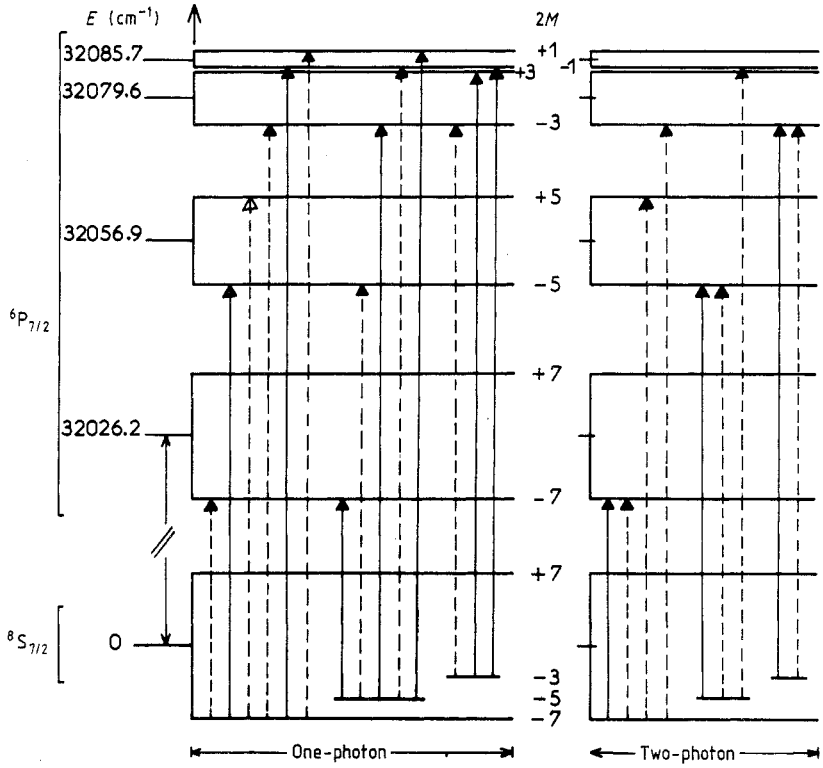

Figure 1. Selection rules for the one- and two-photon $^8S_{7/2}(M) \rightarrow {}^6P_{7/2}(M')$ transitions of the Gd^{3+} ion in $Gd(OH)_3$ with an external magnetic field applied along the c axis: broken and full lines are related to the σ and π polarisations, respectively.

expect four lines for $\varepsilon \| c$. Only three among them are observed because the highest energy line $^8S_{7/2}$ $(M = -\frac{1}{2}) \rightarrow {}^6P_{7/2}$ $(M' = -\frac{1}{2})$ is strongly affected by the population factor and is missing (figure 2). In addition, a weak line occurs at the position of the one-photon transition $^8S_{7/2}$ $(M = -\frac{7}{2}) \rightarrow {}^6P_{7/2}$ $(M' = -\frac{5}{2})$. A greater number of lines (figure 2) appears in the perpendicular polarisation due to the effect of the selection rule $\Delta M = 2$, in addition to $\Delta M = 0$ (figure 1). As seen earlier, all the expected lines are observed except the one arising from the state $M = -\frac{1}{2}$ of the ground term. The same $\Delta M = 1$ extra line observed in the parallel polarisation is also present in this spectrum. Furthermore, a line attributed to the transition $^8S_{7/2}$ $(M = -\frac{7}{2}) \rightarrow {}^6P_{7/2}$ $(M' = +\frac{5}{2})$, appears. The identifications of all these lines are in complete agreement with our one-photon measurements. The intensities of the main lines are listed in table 2. Finally, it is interesting to note that all the lines attributed to transitions starting from $(M = -\frac{7}{2})$ the ground state are extremely narrow while the other lines are considerably broadened as a consequence of ion–ion interaction, a fact which we will discuss in the last section.

3. Analysis of $^8S_{7/2} \rightarrow {}^6P_{7/2}$ two-photon transition intensities

3.1. Theoretical background

In the case of the $^8S_{7/2} \rightarrow {}^6P_{7/2}$ two-photon transitions induced by single-beam excitation with polarisation vector $\boldsymbol{\varepsilon}$, the operator to be placed between the initial state $|g\rangle$ and

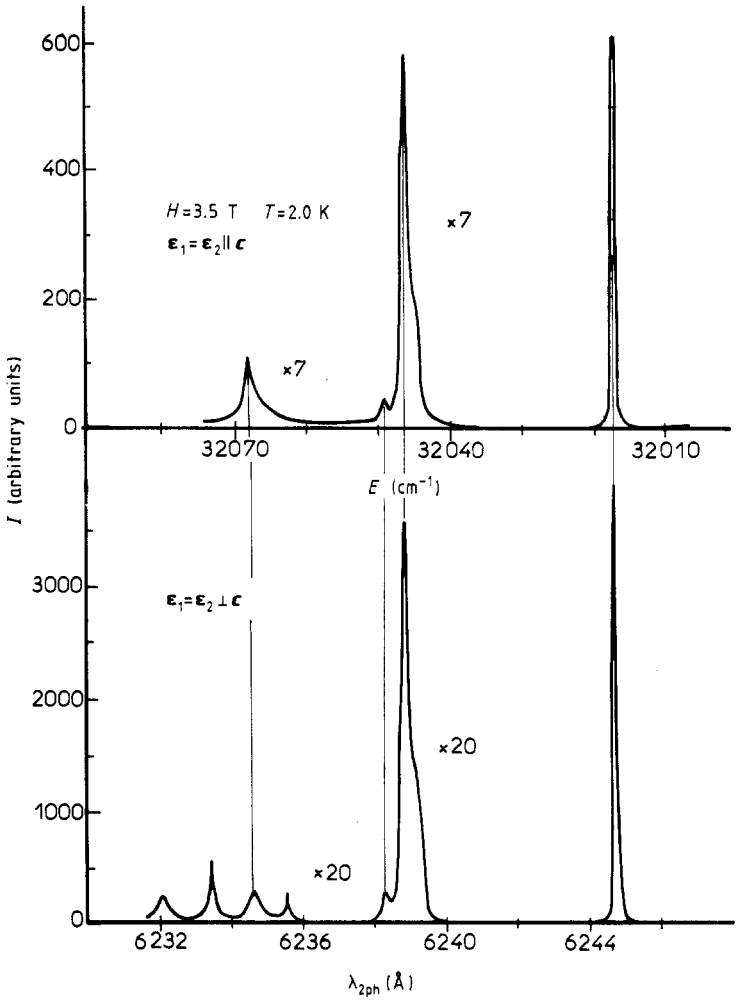

Figure 2. Two-photon excitation spectra of the overall UV fluorescence of $Gd(OH)_3$ with an external magnetic field applied along the c axis.

final state $|u\rangle$ belonging to the $^8S_{7/2}$ and $^6P_{7/2}$ multiplets, respectively, can be recast in the form (Judd and Pooler 1982, Downer and Bivas 1983)

$$3E_{df}^{-1}\left(\tfrac{2}{35}\right)^{1/2}\{\boldsymbol{\varepsilon}^{(1)}\boldsymbol{\varepsilon}^{(1)}\}^{(2)}\cdot\mathbf{U}^{(2)} + 2\left(\tfrac{1}{1400}\right)^{1/2}E_{df}^{-2}(9\zeta_f - 4\zeta_d)\{\boldsymbol{\varepsilon}^{(1)}\boldsymbol{\varepsilon}^{(1)}\}^{(2)}\cdot\mathbf{W}^{(11)2}$$
$$- 2\left(\tfrac{2}{21}\right)^{1/2}E_{df}^{-2}(9\zeta_f + \zeta_d)(\boldsymbol{\varepsilon}^{(1)}\cdot\boldsymbol{\varepsilon}^{(1)})\mathbf{W}^{(11)0} \qquad (1)$$

where E_{df} is the average energy of the $4f^65d$ configuration above the single-photon energy, and ζ_d and ζ_f stand for the spin–orbit coupling constants for d and f electrons.

The first term in (1) represents the standard second-order contribution involving the usual $\mathbf{U}^{(2)}$ Racah unit tensor. The second and third terms constitute the third-order contribution when taking account of the spin–orbit interaction within the $4f^65d$ intermediate states. $\mathbf{W}^{(11)0}$ and $\mathbf{W}^{(11)2}$ are double-tensor operators of spin rank 1, orbital rank 1, and total ranks 0 and 2, respectively (see Judd 1963).

Table 2. Experimental and calculated relative intensities of the $^8S_{7/2}(M) \rightarrow {}^6P_{7/2}(M')$ two-photon transitions in an applied magnetic field of 3.5 T at 2 K. $S^{(2)}_{TPA}$ and $S^{(3)}_{TPA}$ stand for the calculated strengths derived from second-order and third-order analysis (equation (3)), respectively.

$^8S_{7/2}$	$^6P_{7/2}$	$\boldsymbol{\varepsilon} \parallel \boldsymbol{c}$			$\boldsymbol{\varepsilon} \perp \boldsymbol{c}$		
M	M'	$S^{(2)}_{TPA}$	$S^{(3)}_{TPA}$	Exp.	$S^{(2)}_{TPA}$	$S^{(3)}_{TPA}$	Exp.
$-\frac{7}{2}$	$-\frac{7}{2}$	23	772	772	5.8	1361	1361
$-\frac{7}{2}$	$-\frac{3}{2}$				2·5	4	6
$-\frac{5}{2}$	$-\frac{5}{2}$	0.1	224	154	0.02	242	102
$-\frac{5}{2}$	$-\frac{1}{2}$				1.1	1.7	3
$-\frac{3}{2}$	$-\frac{3}{2}$	0.05	15	32	0.013	13	12
$-\frac{3}{2}$	$-\frac{7}{2}$				0.03	0.05	—
$-\frac{3}{2}$	$+\frac{1}{2}$				0.09	0.14	—
$-\frac{1}{2}$	$-\frac{1}{2}$	0.015	2.1	—	0.004	1.4	—
$-\frac{1}{2}$	$-\frac{5}{2}$				0.007	0.011	—
$-\frac{1}{2}$	$+\frac{3}{2}$				0.01	0.016	—

Due to the weakness of crystal-field interactions in $Gd(OH)_3$, J may be assumed to remain a good quantum number (Meltzer and Moor 1972). Moreover, the C_{3h} symmetry of the Gd^{3+} sites in this material is such that only B^6_6 terms can mix M_J values. Since the application of a magnetic field along the direction of the c axis does not induce any additional M_J-mixing, we can start with $|g\rangle$ and $|u\rangle$ states of the form

$$|g\rangle = |4f^7[^8S_{7/2}]M\rangle \qquad |u\rangle = |4f^7[^6P_{7/2}]M'\rangle \tag{2}$$

where the square brackets mean that the states under question are to be understood in the intermediate coupling scheme. Thus, taking a linearly polarised beam with $\boldsymbol{\varepsilon}$ parallel to the c axis ($\boldsymbol{\varepsilon} \parallel \boldsymbol{c}$) we find the strength of the two-photon transition between $|g\rangle$ and $|u\rangle$ states to be proportional to

$$\begin{aligned}
&\tfrac{4}{21}E_{df}^{-2}\Bigg|\tfrac{1}{10}\begin{pmatrix}\frac{7}{2} & 2 & \frac{7}{2}\\ -M & 0 & M'\end{pmatrix}\{6(5)^{1/2}(4f^7[^8S_{7/2}]\|\mathbf{U}^{(2)}\|4f^7[^6P_{7/2}])\\
&\quad + E_{df}^{-1}(9\zeta_f - 4\zeta_d)(4f^7[^8S_{7/2}]\|\mathbf{W}^{(11)2}\|4f^7[^6P_{7/2}])\}\\
&\quad - (2)^{1/2}E_{df}^{-1}(9\zeta_f + \zeta_d)\\
&\quad \times \begin{pmatrix}\frac{7}{2} & 0 & \frac{7}{2}\\ -M & 0 & M'\end{pmatrix}(4f^7[^8S_{7/2}]\|\mathbf{W}^{(11)0}\|4f^7[^6P_{7/2}])\Bigg|^2
\end{aligned} \tag{3a}$$

in agreement with (5c) in the work of Downer and Bivas (1983), and the analogous expression for $\boldsymbol{\varepsilon} \perp \boldsymbol{c}$ is

$$\begin{aligned}
&\tfrac{4}{21}E_{df}^{-2}\Bigg|\tfrac{1}{10}(\tfrac{3}{2})^{1/2}\Bigg[-(\tfrac{1}{6})^{1/2}\begin{pmatrix}\frac{7}{2} & 2 & \frac{7}{2}\\ -M & 0 & M'\end{pmatrix} + \tfrac{1}{2}e^{i2\varphi}\begin{pmatrix}\frac{7}{2} & 2 & \frac{7}{2}\\ -M & -2 & M'\end{pmatrix}\\
&\quad + \tfrac{1}{2}e^{-i2\varphi}\begin{pmatrix}\frac{7}{2} & 2 & \frac{7}{2}\\ -M & 2 & M'\end{pmatrix}\Bigg]\{6(5)^{1/2}(4f^7[^8S_{7/2}]\|\mathbf{U}^{(2)}\|4f^7[^6P_{7/2}])\\
&\quad + E_{df}^{-1}(9\zeta_f - 4\zeta_d)(4f^7[^8S_{7/2}]\|\mathbf{W}^{(11)2}\|4f^7[^6P_{7/2}])\}
\end{aligned}$$

$$- (2)^{1/2} E_{df}^{-1} (9\zeta_f + \zeta_d)$$
$$\times \begin{pmatrix} \frac{7}{2} & 0 & \frac{7}{2} \\ -M & 0 & M' \end{pmatrix} (4f^7[^8S_{7/2}] \| \mathbf{W}^{(11)0} \| 4f^7[^6P_{7/2}]) \Big|^2 \qquad (3b)$$

where φ stands for the polar coordinate of $\boldsymbol{\varepsilon}$ in the xy plane (perpendicular to the c axis).

From the above equations, it is clear that only $\Delta M_J = 0$ transitions should be observed for $\boldsymbol{\varepsilon} \| \mathbf{c}$, while, in addition, $\Delta M = 2$ transitions should appear for $\boldsymbol{\varepsilon} \perp \boldsymbol{c}$. In a first approximation, we can neglect the M_J mixing due to the B_6^6 terms in the crystal-field operator, as assumed by Meltzer and Moos (1972). Then, (3*a*) and (3*b*) lead straightforwardly to the strengths of the individual Stark-components observed when the magnetic field is applied. Since the $^8S_{7/2}$ splitting in zero-field is not resolved, the expressions in (3*a*) and (3*b*) have to be summed over M to obtain the Stark-component intensities in the zero-field spectrum.

3.2. *Comparison with experiment*

Using the numerical values of the spin–orbit coupling constants $\zeta_f = 2\zeta_d = 1500\ cm^{-1}$, the average energy of the excited configuration $4f^6 5d^1$, $E_{df} = 150\,000\ cm^{-1}$ (Downer and Bivas 1983) and the reduced matrix elements of $\mathbf{U}^{(2)}$, $\mathbf{W}^{(11)0}$, $\mathbf{W}^{(11)2}$ (Judd and Pooler 1982, Downer and Bivas 1983, Downer *et al* 1988) we have completed intensity calculations including second- and third-order terms. Experimental and calculated relative intensities have been compiled for both linear polarisations in tables 1 and 2.

As a general feature, calculated intensities of the transitions must include third-order terms to reproduce satisfactorily the relative strength of the Stark components. This is well illustrated for the data obtained in the presence of an external magnetic field (table 2). As an example the intensity ratios between the two lowest components ($M = M' = -\frac{7}{2}$ and $M = M' = -\frac{5}{2}$) are respectively 8 and 14 for the two polarisations including third-order terms while factors of 50 are calculated for the second-order contribution. These values have to be compared to the experimental ones 5 and 13 respectively. A similar behaviour is found for higher crystal-field states, such as $M' = -\frac{3}{2}, -\frac{1}{2}$ with much less accuracy due to the weakness of the lines arising from the depletion of the low-spin states of the $^8S_{7/2}$ ground multiplet. It is then remarkable to note that intensities of the transitions fulfilling the selection rule condition $\Delta M = 2$, observed only in perpendicular polarisation, are well reproduced by second order analysis (table 2).

Downer and Bivas (1983) noticed that interference effects occur because of the sign of the third-order scalar term with respect to the two second-rank contributions. Furthermore the type and degree of interference depend upon the value of M' and on the polarisation. However, in the case of the $^8S_{7/2} \rightarrow {}^6P_{7/2}$ transitions, this effect is shown to be small because of the relative strengths of the scalar and second-order terms.

An interesting feature of the experimental spectra recorded with an applied magnetic field is the presence of a weak line attributed to the normally forbidden transitions $^8S_{7/2}$ $(M = -\frac{7}{2}) \rightarrow {}^6P_{7/2}$ $(M' = +\frac{5}{2})$ (Jacquier *et al* 1987). Within the ^6P manifold the crystal field parameter of rank 6, B_6^6, required in C_{3h} site symmetry allows a small admixture of states among the pairs of M': $-\frac{7}{2}$, $+\frac{5}{2}$ and $+\frac{7}{2}$, $-\frac{5}{2}$. The attribution of this line has been checked by measuring its magnetic field dependence at intermediate field up to 3.5 T. Its intensity provides a convincing test of the extent of the mixing. By comparing the intensity of this line and the one observed for $M = -\frac{7}{2} \rightarrow M' = -\frac{7}{2}$, we

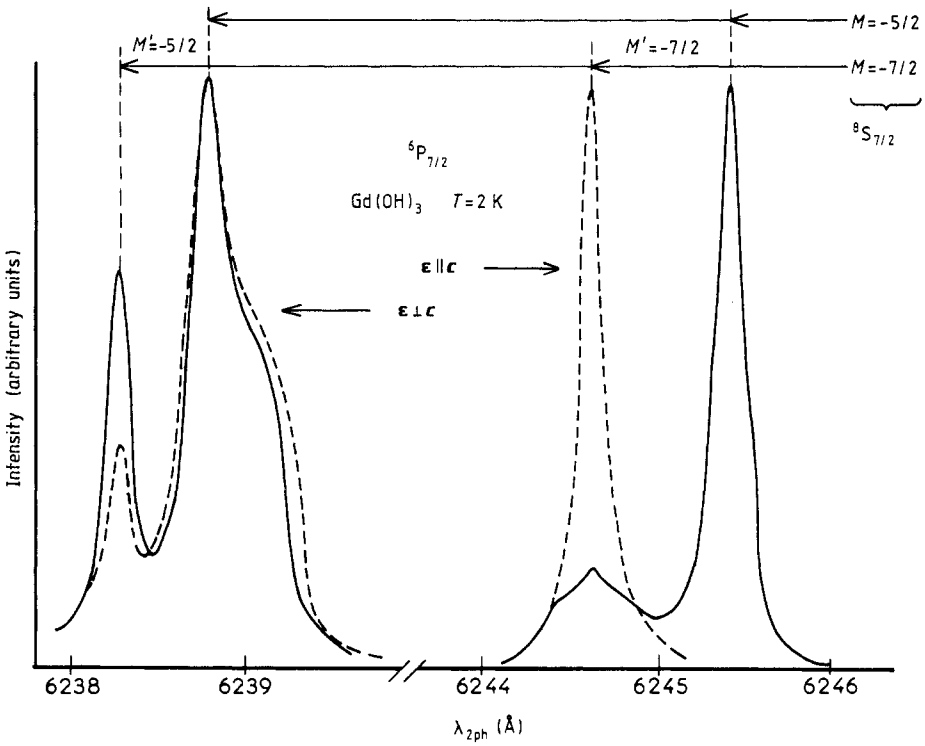

Figure 3. Excitation spectra corresponding to the transitions $^8S_{7/2}$ ($M = -\frac{7}{2}, -\frac{5}{2}$) → $^6P_{7/2}$ ($M' = -\frac{7}{2}, -\frac{5}{2}$) with an external magnetic field of 3.5 T applied along the c axis: full and broken lines represent the one-photon and two-photon spectra, respectively.

measured the square of the admixture coefficient. This leads to a value of 5% mixing of $M' = -\frac{7}{2}$ into $M' = +\frac{5}{2}$. One may ask why this line only appears in the excitation spectrum with perpendicular polarisation (figure 2). A quick calculation shows that the intensity of this line is too weak to be observed on the scale of the parallel polarised excitation spectrum; it should appear in the tail of the broadened line attributed to the transition $M = -\frac{3}{2} \rightarrow M' = -\frac{3}{2}$.

A puzzling question is the appearance of the weak line seating at the energy of the transition $^8S_{7/2}$ ($M = -\frac{7}{2}$) → $^6P_{7/2}$ ($M' = -\frac{5}{2}$) (Salem *et al* 1989) which is normally forbidden as a result of the selection rule $\Delta M = 0, 2$. Experimental arguments may be considered, based on either a slight depolarisation of the laser beam due to the transmission through the windows of the cryostat and reflexion, or a misalignment of the sample into the cooled magnet. The intensity of this line relative to the nearest one attributed to the transition $M = -\frac{5}{2} \rightarrow M' = -\frac{5}{2}$ does not change appreciably with the polarisation (figure 2). Furthermore we already observed a depolarisation for the one-photon experiment. The left-hand side of figure 3 compares the measurements of the transition $M = -\frac{7}{2} \rightarrow M' = -\frac{5}{2}$ which should appear neither in two-photon nor in one-photon spectra for $\boldsymbol{\varepsilon} \perp \boldsymbol{c}$ in the one-photon analysis. As a matter of fact the right-hand side of figure 3 reproduces among other features the one-photon transition $M = -\frac{7}{2} \rightarrow M' = -\frac{7}{2}$, which indicates also a non-negligible depolarisation. The only explanation

which holds for all the above observations would involve a slight crystallographic disorder of the material and perhaps the presence of domains. This misorientation could affect the adequacy of the selection rules ΔM for both one- and two-photon spectra.

4. Concluding remarks

It has been shown that ion–ion exchange interaction involving ground and excited states of nearby optically active ions may strongly affect the optical spectra of rare earth insulators (see for a review, Cone and Meltzer 1987). Exciton band effects have been demonstrated in $GdCl_3$ by Meltzer and Moos (1972). Indeed spectral shift as well as broadening of the lines have been analysed within a framework of an exciton representation using a two sublattice model developed for $GdCl_3$ as well as for the isostructural $Gd(OH)_3$ when an external magnetic field is applied along the easy axis of magnetisation, providing a spin configuration of a ferromagnet. Furthermore, measured exchange splittings of Gd^{3+} in $GdCl_3$ have been used in connection with fundamental two-electron tensor operator description of the electronic exchange interactions to derive the contributions due to dynamic exchange (or matrix element of energy transfer) and the magnetic dipole–dipole interactions (Meltzer and Cone 1976). Our two-photon experiments are shown to be fully consistent with the previous one-photon data and allow us to measure the spectral width of the pure electronic transition $M = -\frac{7}{2} \rightarrow M' = -\frac{7}{2}$ at $k = 0$ ($0.7\ cm^{-1}$).

The left-hand side of figure 3 reports the comparison of the one-photon (σ polarised) and two-photon excitation spectra for the transition $M = -\frac{5}{2} \rightarrow M' = -\frac{5}{2}$. In this last spectrum, the square root of the fluorescence intensity has been plotted so that the same number of incident photons be involved in both cases. The asymmetrical lineshape has been considered to be the result of a convolution of a small dispersion of the excited state ($M' = -\frac{5}{2}$) and of a quite large dispersion of the magnetic excitation in the ground state ($M = -\frac{5}{2}$) with high density of states points occurring mainly at the zone edge of the Brillouin zone. We then observe quite good agreement between the two measurements for both positions and profiles. It is interesting to note that one-photon absorption (Meltzer and Moos 1972) and excitation (Salem *et al* 1989) results, and two-photon excitation data converge to the description of a broadening of the line due to ion–ion interactions. This is also fully consistent with $GdCl_3$ (Mahiou *et al* 1984) where the up conversion fluorescence ($^6I_{7/2} \rightarrow {}^8S_{7/2}$) was used to probe the lineshape. This is an indication that resonant energy transfer among intrinsic ions or coherent motion of the exciton is taking place within a faster scale than other relaxation processes: sensitised fluorescence and up conversion energy transfer.

Finally an interesting feature is the observation of the pure electronic transition $M = -\frac{7}{2} \rightarrow M' = -\frac{7}{2}$ occurring at $k = 0$. Figure 3 (right-hand side) reports the position and the shape of that line compared to the one-photon magnon–exciton transition $M = -\frac{5}{2} \rightarrow M' = -\frac{7}{2}$. We were able to measure a half-height width of $0.7\ cm^{-1}$ while the laser bandwidth was smaller than $0{\cdot}1\ cm^{-1}$. This halfwidth was not measurable in one-photon absorption or excitation spectra because the exciton line was always saturated. The broadening of this line correlates well the hopping time scale which can be derived from fluorescence dynamics of isotype magnetic insulators $GdCl_3$ (Mahiou *et al* 1988) and $Gd(OH)_3$ (Salem *et al* 1989).

Acknowledgments

We wish to thank Dr S Mroczkowski for providing us the crystal used in this work. We acknowledge helpful discussions with Dr R Mahiou (Université de Clermont II) and Professor R S Meltzer (University of Georgia). Partial support by NATO under contract No 84/0505 is also gratefully acknowledged.

References

Cone R L and Meltzer R S 1987 *Spectroscopy of Solids Containing Rare Earth Ions, Modern Problems in Condensed Matter Sciences,* vol 27, ed. A A Kaplyanskii and R M Macfarlane (Amsterdam: North-Holland) pp 481–556

Dagenais M, Downer M, Neuman R and Bloembergen N 1981 *Phys. Rev. Lett.* **46** 561–5

Downer M C and Bivas A 1983 *Phys. Rev.* B **28** 3677–96

Downer M C, Burdick G W and Sardar D K 1988 *J. Chem. Phys.* **89** 1787–97

Jacquier B, Salem Y, Linares C, Gacon J C, Mahiou R and Cone R L 1987 *J. Lumin.* **38** 258–60

Judd B R 1963 *Operator Techniques in Atomic Spectroscopy* (New York: McGraw-Hill)

Judd B R and Pooler D R 1982 *J. Phys. C: Solid State Phys.* **15** 591–8

Mahiou R, Jacquier B and Linares C 1983 *J. Opt. Soc. Am.* **73** 1383

Mahiou R, Jacquier B and Madej C 1988 *J. Chem. Phys.* **89** 5931

Mahiou R, Jacquier B and Moncorge R 1984 *Proc. Rare Earth Symposium* (Singapore: World Scientific)

Meltzer R S and Cone R L 1976 *Phys. Rev.* B **13** 2818–30

Meltzer R S and Moos H W 1972 *Phys. Rev.* B **6** 264–77

Mroczkowski S, Eckart J, Meissner H F and Doran J C 1970 *J. Cryst. Growth* **6** 477–85

Salem Y, Jacquier B, Mahiou R and Cone R L 1989 unpublished

Skjeltorp A T, Catanese C A, Meissner H F and Wolf W P 1972 *Phys. Rev.* B **7** 2062–91